SUPPLEMENTARY INFORMATION

Table S1. Model parameters for tracer kinetic modeling of MM-DX-929 liposome transport into and out of tumors.

Parameter	Description	Value	Units	Reference
V_c	Blood volume	Fit to data	L	
k_{el}	Rate constant for elimination of liposome from blood	Fit to data	1/min	
V_t	Tumor volume	From images	L	
VVF	Vascular volume fraction		Dimensionless	
Q	Blood flow rate into tumor per unit tissue	0.212	L/min/kg	(1)
ρ	Tissue density	1	kg/L	
k_1	Permeability surface area product per unit tissue for transport from tumor capillary into tumor tissue	Fit to data	L/min/kg	
k_{-1}	Permeability surface area product per unit tissue for transport out of tumor tissue into tumor capillary	Fit to data	L/min/kg	

Model equations:

$$\frac{dC_b}{dt} = \frac{1}{V_c}(-k_{el} \cdot C_b \cdot V_c - Q \cdot V_t \cdot \rho \cdot C_b + Q \cdot V_t \cdot \rho \cdot C_{tv})$$

$$\frac{dC_{tv}}{dt} = \frac{V_t \cdot \rho}{V_t \cdot VVF}(Q \cdot C_b - Q \cdot C_{tv} - k_1 \cdot C_{tv} + k_{-1} \cdot C_{tt})$$

$$\frac{dC_{tt}}{dt} = \frac{V_t \cdot \rho}{(1 - VVF)}(k_1 \cdot C_{tv} - k_{-1} \cdot C_{tt})$$

$$C_{t,total} = C_{tv} \cdot VVF + C_{tt} \cdot (1 - VVF)$$

where C_b, C_{tv}, C_{tt}, $C_{t,total}$ are the concentrations of MM-DX-929 in the blood, tumor vasculature, tumor tissue, and total tumor compartment, respectively.

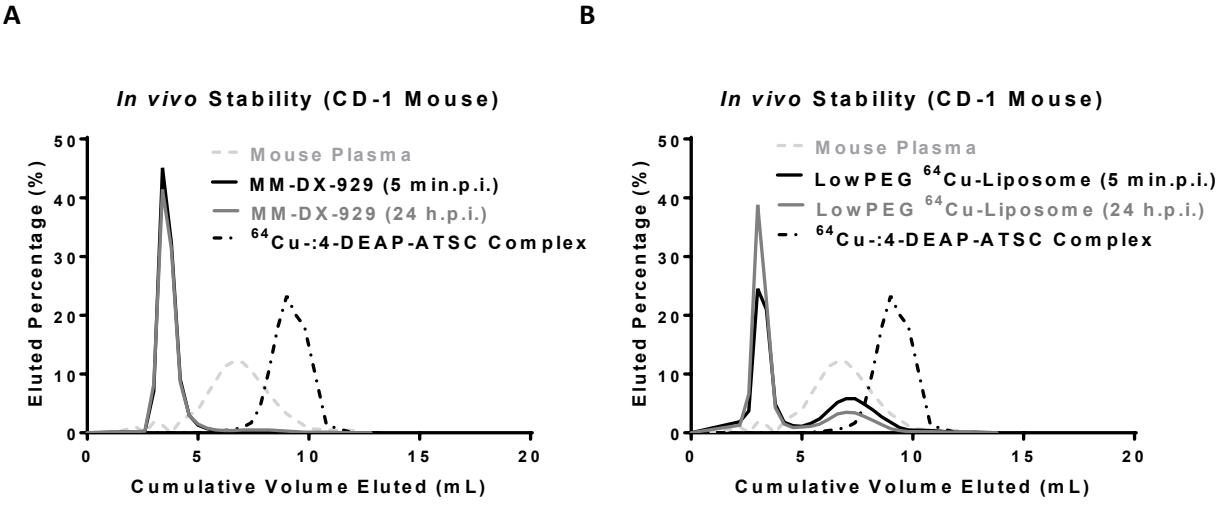

Figure S1. ***In vivo*** **Stability of MM-DX-929 in immunocompetent CD-1 Mouse.** Sepharose CL4B columns were characterized using fluorescently-labeled liposomes, mouse plasma, or free ^{64}Cu:4-DEAP-ATSC complex to determine the fractions at which liposome, plasma protein, or released ^{64}Cu:4-DEAP-ATSC elute, respectively. Free ^{64}Cu is retained within the column with < 3% of recovery from elution at 100 mL of cumulative volume. Plasma (dotted grey line) and free ^{64}Cu:4-DEAP-ATSC fractions (dotted black line) were identified using UV-vis absorbance at 280 nm and gamma-counter, respectively. Following intravenous injection of **(A)** MM-DX-929 (10 mol%) or **(B)** low PEGylation ^{64}Cu-liposome (0.5 mol%), blood was collected from the mice at 5 mins or 24 hours post-injection via saphenous vein. Plasma samples were loaded onto the columns to separate the liposomal ^{64}Cu from released ^{64}Cu.

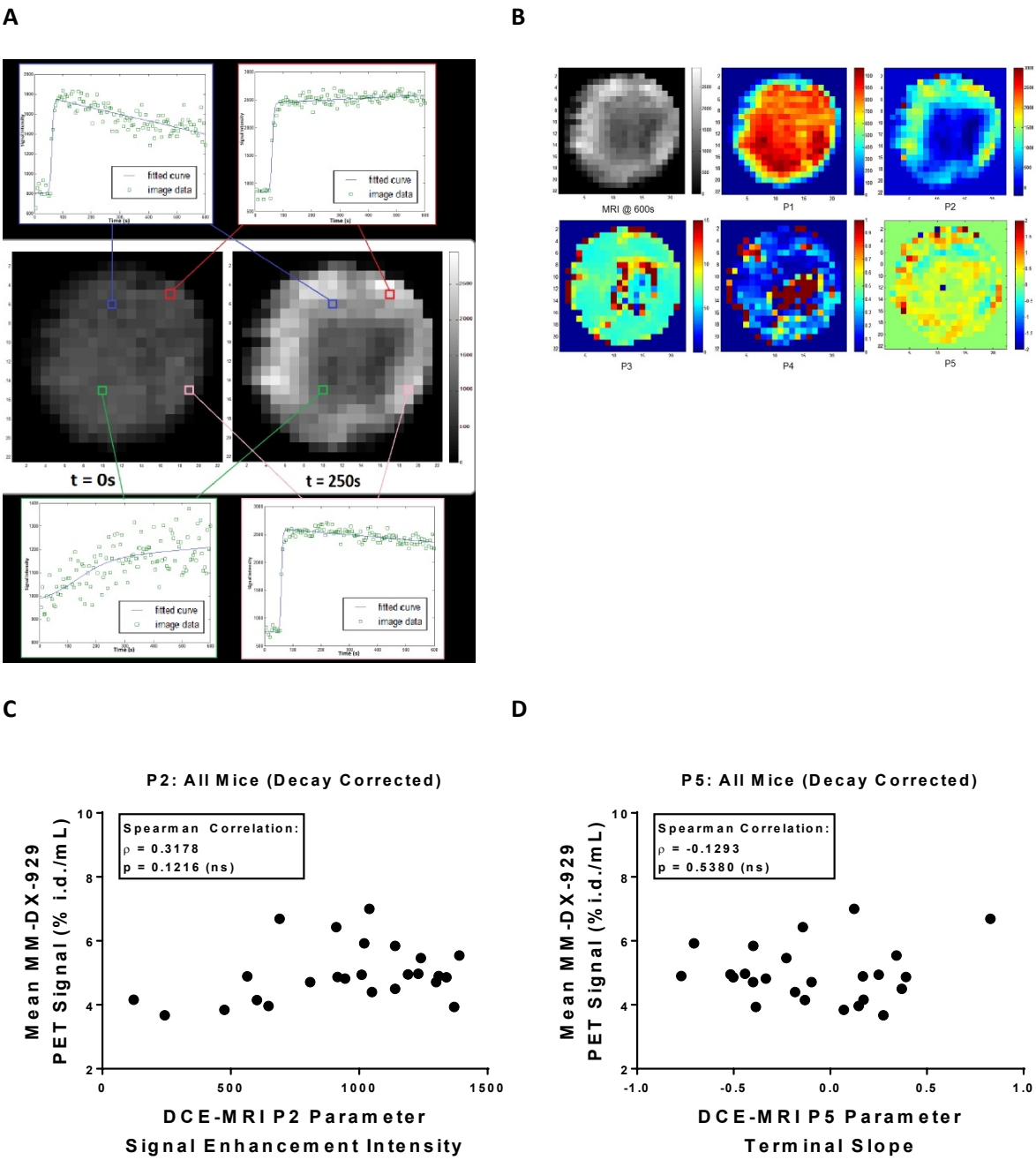

Figure S2. DCE-MRI derived contrast accumulation kinetics does not correlate with MM-DX-929 tumor deposition quantified by PET. Mice bearing BT474-M3 orthotopic mammary fat pad tumors were injected with MM-DX-929 intravenously. At 24 h.p.i., mice underwent PET/CT image acquisition follow procedures described in Materials and Methods. Immediately following PET/CT imaging, mice were transferred to a 1T MRI system (M3, Aspect Imaging; Shoham, Israel) and received a bolus intravenous injection of a clinically used MR contrast agent (gadoteridol, Prohance®; Bracco, Italy). A T1-weighted dynamic imaging sequence was acquired over 10 mins with a temporal resolution of 5 s starting at 10 s

prior to MR contrast injection. A multi-parametric logistic kinetic model described by Moate *et al.* was used to analyze the DCE-MRI data (2). Specifically, each tumor voxel from the DCE-MRI dataset was fit to the following equation **(A)**: $Signal\ Intensity(t) = \frac{P_2 + P_5 \cdot t}{\{1+\exp(-P_4 \cdot (t-P_3))\}} + P_1$ **(B)** Five parametric tumor maps were generated to represent each of the five kinetic parameters. In particular, **(C)** P2 and **(D)** P5 parameters, representing contrast enhancement and clearance kinetics, respectively, were selected as relevant parameters for determining correlation with MM-DX-929 tumor deposition obtained from PET images.

REFERENCES FOR SUPPLEMENTARY INFORMATION

1. Baxter LT, Zhu H, Mackensen DG, Jain RK. Physiologically based pharmacokinetic model for specific and nonspecific monoclonal antibodies and fragments in normal tissues and human tumor xenografts in nude mice. Cancer Res. 1994;54:1517–28.

2. Moate PJ, Dougherty L, Schnall MD, Landis RJ, Boston RC. A modified logistic model to describe gadolinium kinetics in breast tumors. Magn Reson Imaging. 2004;22:467–73.